



# High Efficiency Graphene Coated Copper Based Thermocells Connected in Series

Mani Sindhuja<sup>1,2</sup>, Emayavaramban Indubala<sup>1,3</sup>, Venkatachalam Sudha<sup>3</sup> and Seshadri Harinipriya<sup>1\*</sup>

<sup>1</sup> Electrochemical Systems Lab, SRM Research Institute, SRM Institute of Science and Technology, Kattankulathur, India,

<sup>2</sup> Department of Physics and Nanotechnology, SRM Institute of Science and Technology, Kattankulathur, India, <sup>3</sup> Department of Chemistry, SRM Institute of Science and Technology, Kattankulathur, India

Conversion of low-grade waste heat into electricity had been studied employing single thermocell or flowcells so far. Graphene coated copper electrodes based thermocells connected in series displayed relatively high efficiency of thermal energy harvesting. The maximum power output of 49.2 W/m<sup>2</sup> for normalized cross sectional electrode area is obtained at 60°C of inter electrode temperature difference. The relative carnot efficiency of 20.2% is obtained from the device. The importance of reducing the mass transfer and ion transfer resistance to improve the efficiency of the device is demonstrated. Degradation studies confirmed mild oxidation of copper foil due to corrosion caused by the electrolyte.

**Keywords:** graphene, copper, thermocells, efficiency, inter electrode temperature

## OPEN ACCESS

### Edited by:

Ramesh L. Gardas,  
Indian Institute of Technology Madras,  
India

### Reviewed by:

Siddharth Surajbhan Gautam,  
The Ohio State University,  
United States  
Ravindra Pandey,  
University of Texas at Austin,  
United States

### \*Correspondence:

Seshadri Harinipriya  
harinipriya.s@res.srmuniv.ac.in

### Specialty section:

This article was submitted to  
Physical Chemistry and Chemical  
Physics,  
a section of the journal  
Frontiers in Physics

**Received:** 08 December 2017

**Accepted:** 03 April 2018

**Published:** 18 April 2018

### Citation:

Sindhuja M, Indubala E, Sudha V and  
Harinipriya S (2018) High Efficiency  
Graphene Coated Copper Based  
Thermocells Connected in Series.  
Front. Phys. 6:35.  
doi: 10.3389/fphy.2018.00035

## INTRODUCTION

Low grade waste heat (i.e., at temperatures <200°C), such as that produced via industrial or geothermal processes, in particular was a significant source of energy that could be harvested for the production of electricity. In the field of wearable devices, where the utilization of body heat could power small portable electronics, such as medical devices or sensors [1, 2], thermocells become inevitable. Thermo-electrochemical cells, are electrochemical devices that produce a steady electric current under an applied temperature difference between two electrodes [3–5]. Due to the dependency of the performance of the cell on the ohmic, charge transfer and mass transport overpotentials [6–8], the performance of a given cell cannot be determined solely from the Seebeck coefficient.

Fast charge transfer property and low resistance at the electrode/electrolyte interface were important factors for an electrode material to determine the electrochemical performance [9]. Pt was usually used as electrode materials in thermocells, and this restricted the commercial viability [10–14]. Carbon-based electrodes were gaining prominence as a promising, low-cost alternative to Pt. The added advantage of carbon electrodes was the fast electron transfer kinetics of Ferri/Ferrocyanide redox couple [1]. Majority of research in this area had been focused on composite materials that incorporate nano-structured materials such as nanotubes, graphene [10, 15–17] and additional treatment of materials via additives or doping [4]. The real time applications of thermocells were extensively limited by its low voltage generation. Although the maximum potential of a single cell was limited by the Seebeck coefficient and the temperature gradient, the potential difference could be increased significantly by connecting the cells in series [1]. The goal of present work is to fabricate cost-effective graphene coated copper based thermocell (3 cells in series) that generate very high power output per unit area and energy conversion

efficiencies to the level at which they can be more efficient than thermoelectric devices for low grade thermal-energy harvesting. To push the utility of thermocells in real-time applications three thermocells are connected in series to take advantage of the increased voltage output. Usage of graphene coated copper improved the energy conversion efficiency via fast redox processes, high thermal and electrical conductivities. Here, we exploit simple dip coating processed graphene coated copper in planar configuration to optimize the carnot efficiency. The optimized strategies include usage of highly thermally and electrically conducting copper metal as base as well as current collector of the device. Graphene coating is used to improve the electron transfer kinetics. The output power density generated by the planar cells in series reached  $49.2 \text{ W/m}^2$  for inter electrode temperature difference of  $60^\circ\text{C}$  and correspond to the relative carnot efficiency of 20.2%. Thus, three thermocells connected in series could harness 20.2% of the maximum energy conversion efficiency possible for a heat engine operating between two given temperatures.

## EXPERIMENTAL DETAILS

XRD patterns of the samples were obtained using PANalytical X-ray diffractometer, Netherlands. Electrochemical impedance measurements were conducted in the frequency range between 100 kHz and 100 mHz using a Zahner Zennium Electrochemical workstation. Cyclic Voltammetry using Zahner Zennium is carried out in aqueous  $1\text{M K}_3[\text{Fe}(\text{CN})_6]$  solution at the scan rate of  $25 \text{ mV/s}$ . Platinum and Ag/AgCl electrodes were used as counter and reference electrodes respectively for the electrochemical measurements.

Three single graphene coated copper thermocells were stacked in series configuration in such a way that the input heat flux from the hotter cell is transferred to the next cell. Illustrative representation of the thermocells were provided in **Figure 1**. For preparation of thermocell electrodes, copper sheet is taken and cut into required shape and cleaned with nitric acid to eliminate contaminants and oxides. Five grams of graphene is mixed well with distilled water in the form of paste. The paste is applied on cleaned copper sheet using paint brush and allowed to dry for 2–3 h. The graphene coated copper electrode with an area of  $1.2 \times 10^{-4} \text{ m}^2$  is used to evaluate thermocell performance. Five grams of Agar-agar powder is mixed in 50 ml of water and  $1\text{M}$  potassium ferricyanide is added to it with constant stirring at  $80^\circ\text{C}$  until formation of gel electrolyte. The electrolyte is sandwiched between two electrodes and sealed with copper leads as current collectors. The device and electrochemical measurements such as Linear Sweep Voltammetry (LSV) and Electrochemical Impedance Spectroscopy (EIS) employed agar-agar gel soaked in aqueous solution of  $1\text{M K}_3[\text{Fe}(\text{CN})_6]$  as electrolyte. Cyclic Voltammetric (CV) measurements used an aqueous solution of  $1\text{M K}_3[\text{Fe}(\text{CN})_6]$  as electrolyte.

## RESULTS AND DISCUSSIONS

To obtain high power generation from the device, fast transport of redox mediator into electrodes is required. The effectiveness

of ion transport in graphene coated copper electrodes is characterized by evaluating the mass transfer coefficient.

### Estimation of Mass Transfer Coefficient

By exploiting the limiting current method, the mass transfer coefficient is estimated [7, 18] from the Equation (1):

$$K_c = i_L/nFAc_\infty \quad (1)$$

where  $i_L$  being the limiting current,  $n = 1$  denote the number of moles of electrons transferred,  $F$  represent the faraday constant ( $96,485 \text{ C/mol}$ ),  $A$  depict the electrode area ( $1.2 \times 10^{-4} \text{ m}^2$ ) and  $C_\infty$  correspond to the bulk species concentration ( $1 \text{ mol/cm}^3$ ). In the present scenario, limiting current as seen from **Figure 2A**, possess negligible current plateau, hence we approximated the maximum current as  $i_L$  to determine  $K_c$ . This approximation might not affect the obtained values as the maximum current is in mA for all scan rates. Hence calculated  $K_c$  may possess about 5% error rather than changing in orders of magnitude.

LSV of the devices based on graphene coated copper from 1 to  $100 \text{ mV/s}$  at  $\Delta T = 60^\circ\text{C}$  are shown in **Figure 2A**. Using Equation (1), the lower limit of the mass transfer coefficient of graphene coated copper based thermocells in series is calculated as  $3.47 \times 10^{-3} \text{ m/s}$ . At  $\Delta T = 60^\circ\text{C}$  as shown in **Figure 2B**, this value is found to be three orders of magnitude higher than that of CNT aerogel sheet ( $5.19 \times 10^{-6} \text{ m/s}$ ) and CNT buckypaper ( $2.51 \times 10^{-6} \text{ m/s}$ ) as reported in the literature [18, 19].

### EIS Analysis

EIS analysis is performed to support the performance improvement. The Nyquist plot of the device at  $\Delta T = 60^\circ$  is recorded employing Zahner Zennium electrochemical workstation and provided in **Figure 3A**. Corresponding bode plots to represent the processes happening in the device due to supply of thermal energy is also provided in **Figure 3B**. The Bode plot showed two time constants (R-Cs) as represented by two regions. The two regions correspond to (i) semicircle at high frequency region (100 kHz–10 Hz) representing charge transfer resistance ( $R_1$ ) (ii) tailing off at low frequency region (10 Hz–100 mHz) indicating mass transfer resistance ( $R_2$ ). The appropriate equivalent circuit model for the nyquist plot is fitted using Zman software ( $R_s-R_1|Q_1-R_2|Q_2$ ) as shown in **Figure 3C**.

For  $\Delta T = 60^\circ\text{C}$ , the series resistance ( $R_s$ ) of the device being  $1.90 \Omega$  and correspond to the resistances at electrode/electrolyte interface which is 5.8 times lower than the series resistance of  $11 \Omega$  for the thermocells fabricated using as drawn, thermally oxidized and Pt-deposited CNT electrodes [18]. The charge transfer resistance ( $R_1$ ) of the device for  $\Delta T = 60^\circ\text{C}$  is  $5.12 \Omega$ , attributed by the electron transfer reaction at electrode/electrolyte interface which is 6 times lower than the charge transfer resistance of  $31 \Omega$  for as drawn, thermally oxidized CNT and 4.5 times lower than that of the charge transfer resistance of  $23 \Omega$  for Pt-deposited CNT electrodes respectively [18]. The mass transfer resistance ( $R_2$ ) for  $\Delta T = 60^\circ\text{C}$  is  $21 \Omega$  and attributed to the transport of Ferro/Ferricyanide ions from bulk to the electrode/electrolyte interface. For  $\Delta T = 60^\circ\text{C}$ , the CPE value,  $Q_{y1} = 5.58 \text{ m}\Omega^{-1}\text{S}^{0.6}$  and its exponent parameter  $Q_{a1} = 0.6$  correspond to diffusion layer capacitance as shown in

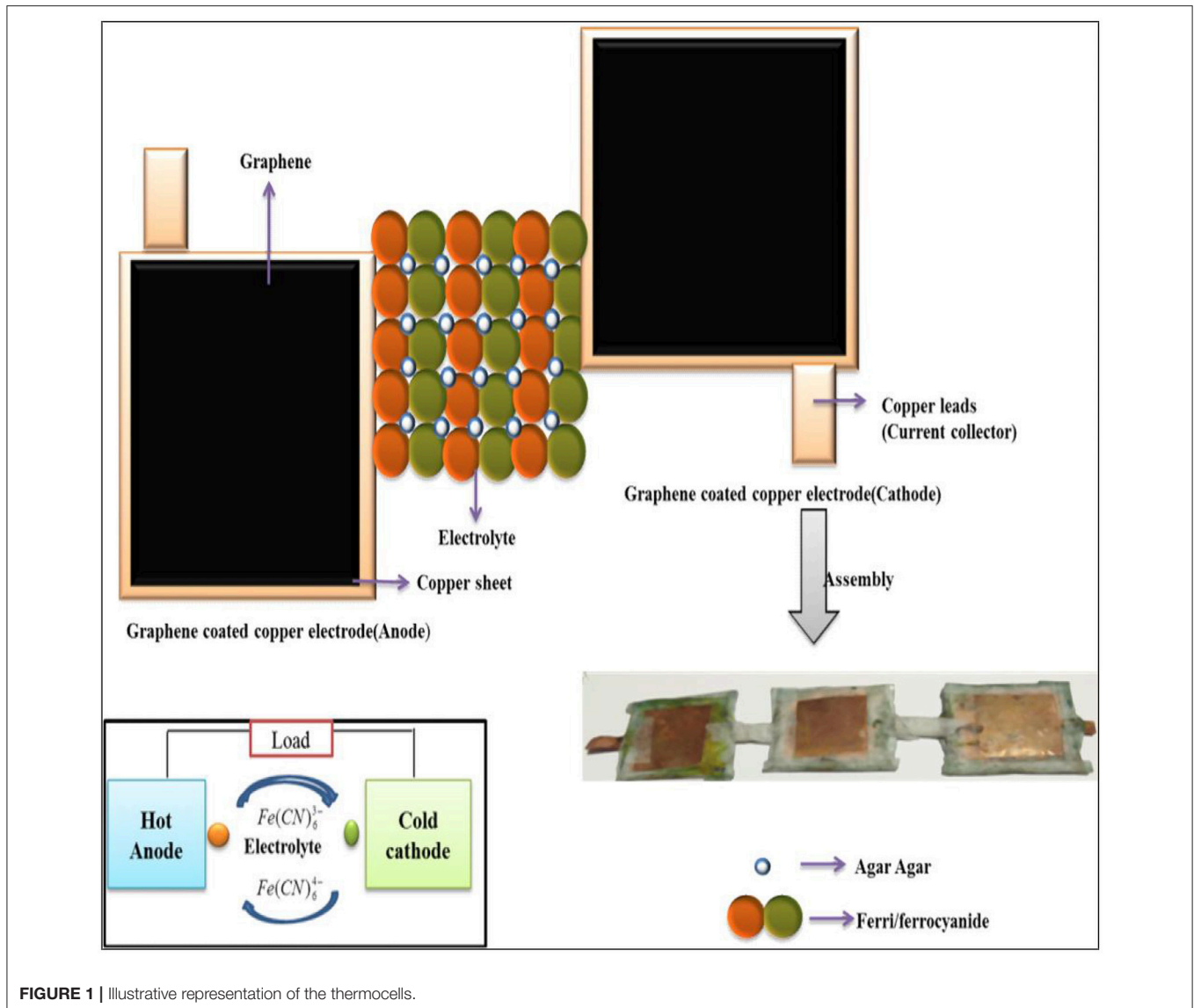


FIGURE 1 | Illustrative representation of the thermocells.

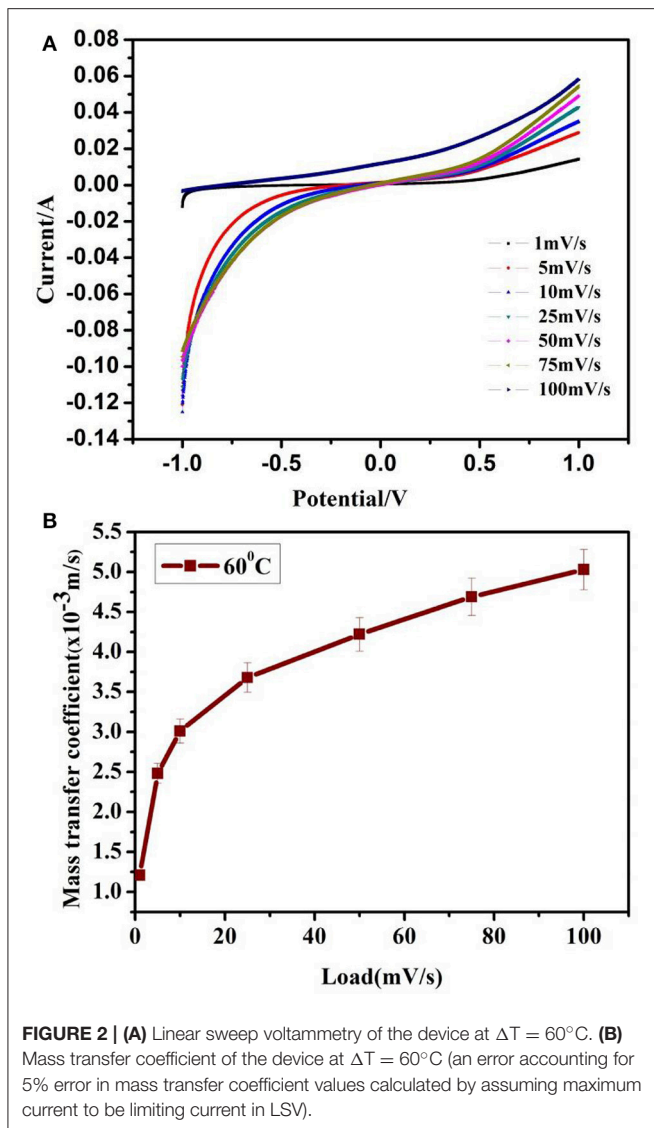
**Figure 3D.**  $Q_{y2} = 27.0 \text{ m } \Omega^{-1} \text{ S}^{0.2}$  and its exponent parameter  $Q_{a2} = 0.2$  could be correlated to the distorted resistance generated during the phononic vibration in the electrode caused by thermal energy as shown in **Figure 3D**.

### Performance of Thermocells Connected in Series

The power from a single thermocell of area  $0.0064 \text{ m}^2$  [19] proved to be insufficient for practical application in small electronic devices like mobile batteries, health care devices, so on and so forth. Therefore, cost effective electrode materials are experimented in a single flat type graphene based thermocell. In order to achieve higher voltage, flat type cells are connected in series and characterized at different temperature gradient ( $\Delta T$ ) (cf. Supplementary Material).

The power and current density variation with load is shown in **Table 1**. The current density ( $j_{sc}$ ) and maximum power density

( $P_{max}$ ) of  $64.6 \text{ A/m}^2$  and  $1.36 \text{ W/m}^2$  respectively, generated by the MWCNT buckypaper electrodes for an optimized electrical load had been the highest among the tested electrode materials, so far [10]. The Pt electrodes generated  $j_{sc}$  of  $48.4 \text{ A/m}^2$  and  $P_{max}$  of  $1.02 \text{ W/m}^2$  [10], the graphite sheet electrodes generated a  $j_{sc}$  of  $36.6 \text{ A/m}^2$  and a  $P_{max}$  of  $0.76 \text{ W/m}^2$ . For a nominal  $\Delta T$  of  $45^\circ\text{C}$ , voltage of  $51.2 \text{ mV}$  and current density stabilized at  $30.4 \text{ A/m}^2$  in the coin like thermocell with buckypaper electrodes were generated. At  $\Delta T = 60^\circ\text{C}$ ,  $V_{oc}$  was  $70.4 \text{ mV}$  and  $j_{sc}$  stabilized at  $55.7 \text{ A/m}^2$  in the coin like thermocell with MWCNT forest electrodes [10]. The power density of  $1.68 \text{ mW/m}^2$  was attained at  $60^\circ\text{C}$  when 5 cells in series with activated charcoal as electrode material was used [20]. In the previous work [19] for single cell, the maximum current and power density obtained were  $0.63 \text{ A/m}^2$ ,  $0.19 \text{ W/m}^2$  at  $\Delta T = 50^\circ\text{C}$  indicating that graphene coated copper could be an efficient electrode system. In this present work for the fabricated series thermocell, the maximum current



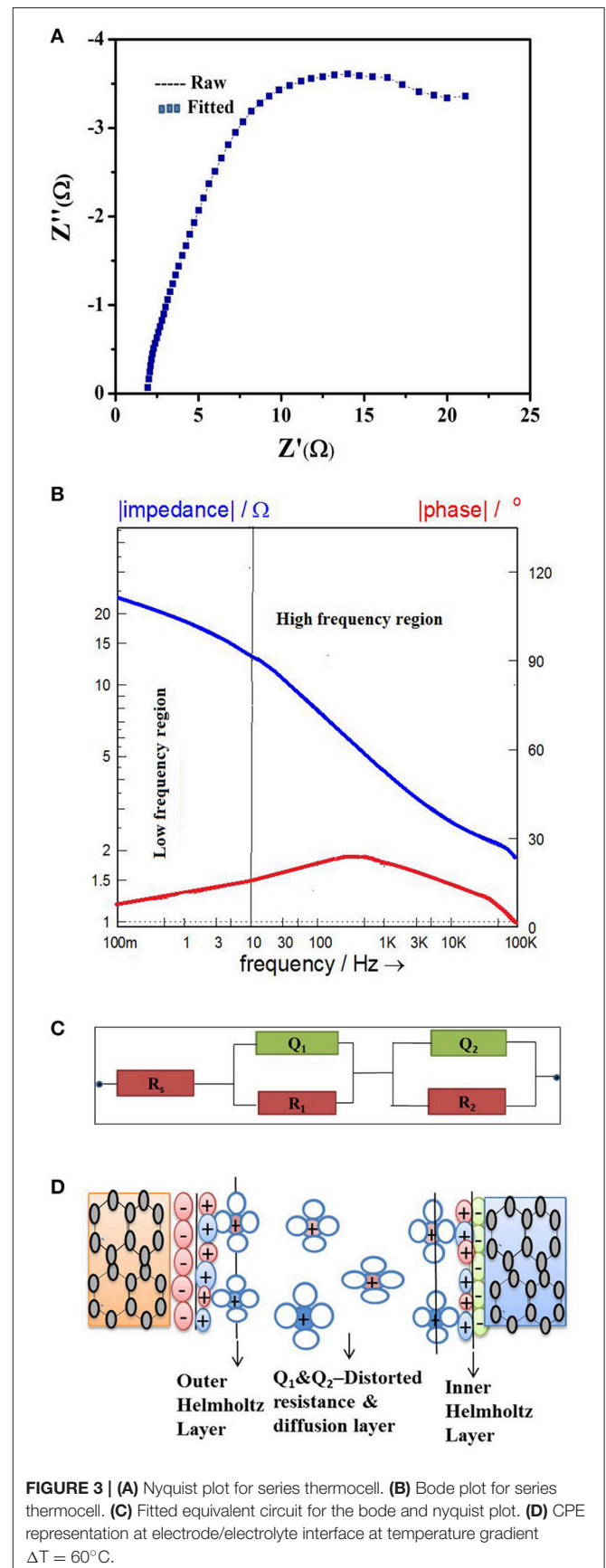
and power density obtained were  $98.3 \text{ A/m}^2$  and  $49.2 \text{ W/m}^2$  at  $\Delta T = 60^\circ\text{C}$ . The power and current density values obtained for series thermocell is much higher than the single thermocell and currently available literature data [10, 19, 20].

The energy conversion efficiency ( $\eta$ ) of the device is given by:

$$\eta = \frac{(1/4)V_{OC} \cdot I_{SC}}{A_c \kappa (\Delta T/d)} \quad (2)$$

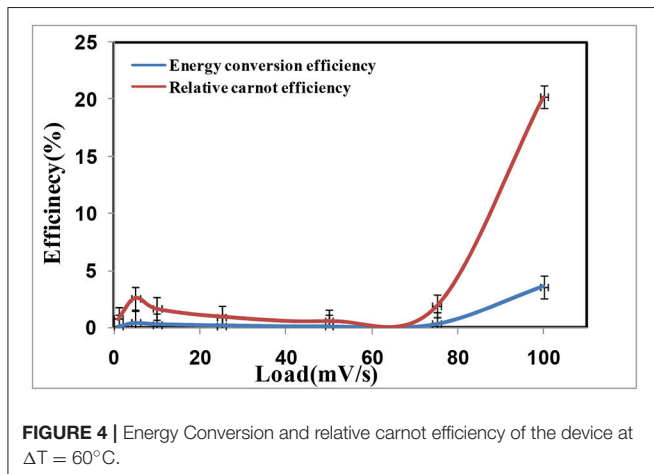
where  $V_{OC}$  denote the open-circuit voltage,  $I_{SC}$  depict the short circuit current,  $A_c$  represented the cross-sectional area of the cell,  $\kappa$  correspond to the thermal conductivity of the electrolyte,  $\Delta T$  indicate the temperature difference between the electrodes and  $d$  being the electrode separation distance.

The energy conversion efficiency is calculated [18] using Equation (2) for different loads at  $\Delta T = 60^\circ\text{C}$  as shown in **Figure 4**. The parameters employed were  $V_{OC} = 0.5 \text{ V}$ ,  $I_{SC} = 11.8 \text{ mA}$ ,  $A = 0.00012 \text{ m}^2$ ,  $\kappa = 0.57 \text{ W/m/K}$ ,  $\Delta T = 60^\circ\text{C}$ ,



**TABLE 1** | Power and current density values of the device at  $\Delta T = 60^\circ\text{C}$ .

Load in mV/s	$J_{sc}$ (mA/m <sup>2</sup> )	$E_{oc}$ (V)	$I_{sc}$ (mA)	$P_{max}$ (mW)	$P_{fmax}/A$ (mW/m <sup>2</sup> )
1	3916.6	0.5	0.47	0.235	1958.3
5	12583.3	0.5	1.51	0.755	6291.6
10	8250.0	0.5	0.99	0.495	4125.0
25	4500.0	0.5	0.54	0.270	2250.0
50	2916.6	0.5	0.35	0.175	1458.3
75	9250.0	0.5	1.11	0.550	4583.3
100	98333.3	0.5	11.8	5.900	49166.6

**FIGURE 4** | Energy Conversion and relative carnot efficiency of the device at  $\Delta T = 60^\circ\text{C}$ .

$d = 10$  cm. It would be clearly seen from **Figure 4**, that the maximum energy conversion efficiency of the fabricated graphene coated copper based thermocell (3 cells in series) to be 3.59% at a load of 100 mV/s for  $\Delta T = 60^\circ\text{C}$  which is 2.5 times higher than graphene based thermocell [19], 134 times higher than the energy conversion efficiency of 0.027% attained at  $60^\circ\text{C}$  when 5 cells in series with activated charcoal as electrode material was used [20], 45 times higher than the energy conversion efficiency of 0.085% at  $60^\circ\text{C}$  attained from flat cell with CNT as electrode material [20], 8.2 times higher than energy conversion efficiency of 0.44% at  $60^\circ\text{C}$  attained from MWCNT based flat thermocells and 6.4 times higher than the maximum energy conversion efficiency of 0.56% attained from cylindrical CNT aerogel sheets based thermocells [18].

The energy conversion efficiency ( $\eta_r$ ), relative to the Carnot efficiency of a heat engine is given by,

$$\eta_r = \eta / (\Delta T / T_H) \quad (3)$$

where  $T_H$  is the hot electrode temperature ( $65^\circ\text{C}$ ).

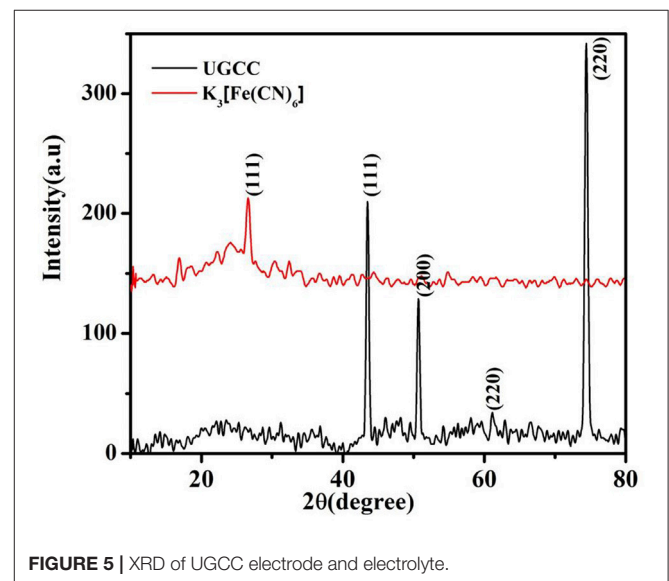
The relative carnot efficiency is calculated using Equation (3) for different load from 1 to 100 mV/s as shown in **Figure 4**. Carnot efficiency of 1.4% was achieved in the literature by employing MWCNTs (multiwall carbon nanotubes) as electrode material with aqueous Ferri/Ferrocyanide redox couple [10]. Upon fabrication of CNT aerogel sheet electrodes, power as high as  $6.6 \text{ W/m}^2$  with a relative carnot efficiency of 3.95% at

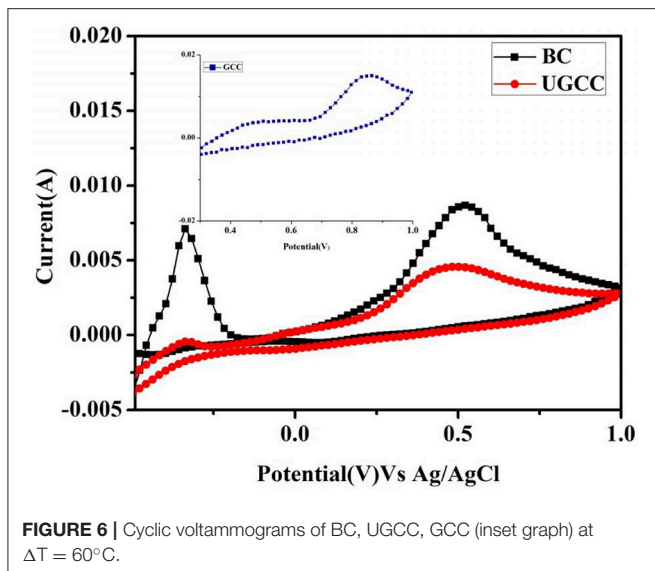
$\Delta T = 51^\circ\text{C}$  had been reported in the literature [18]. Carnot efficiency of 0.98% attained at  $60^\circ\text{C}$  for 5 cells in series with activated charcoal as electrode material [20]. It could be clearly seen from **Figure 4**, that the resulting maximum relative carnot efficiency to be  $\eta_r = 20.2\%$  at  $\Delta T = 60^\circ\text{C}$  for fabricated graphene based thermocell (3 cells in series) which is 12.9 times higher than the single cell graphene based thermocell [19] and 20.7 times higher than activated charcoal based devices reported in the literature [20].

## Degradation Studies

As the solvent used in the present study is water which boils at and above  $60^\circ\text{C}$ , beyond  $\Delta T = 60^\circ\text{C}$ , water vapor accumulation starts happening inside the device. Due to this, cell opening and loss of thermal energy via absorption by water vapor and oxidation of copper reduces the performance of the device. Thus, after  $\Delta T = 60^\circ\text{C}$  sudden decline in the efficiency of the device is noticed. Degradation analysis of the bare copper (BC), used graphene coated copper (UGCC) were studied employing X-ray diffraction and CV before and after the performance studies of the thermocells.

The source consisted of Cu  $K\alpha$  radiation ( $\lambda = 1.54 \text{ \AA}$ ). Three peaks centered at  $43.4^\circ$ ,  $50.7^\circ$ , and  $74.4^\circ$  assigned to (111), (200), and (220) crystal planes of metallic copper, could be clearly observed in the XRD pattern of UGCC electrode as shown in **Figure 5** [21–23]. It also showed the presence of peaks due to the formation of  $\text{Cu}_2\text{O}$  on the electrode surface. The low peak intensity at  $2\theta = 61.1^\circ$  correspond to the  $\text{Cu}_2\text{O}$  (JCPDS 78-2076) which confirmed the oxidation of copper foil due to corrosion [21, 22]. The XRD pattern of agar-Ferro/Ferricyanide electrolyte used as shown in **Figure 5** indicated peaks at  $2\theta$  values of  $26.6^\circ$  corresponding to Ferro/Ferricyanide [24] and peak at  $17.0^\circ$  corresponds to agar film [25, 26] which confirmed the presence of electrolyte without any degradation. Thus, the corrosion of copper foil

**FIGURE 5** | XRD of UGCC electrode and electrolyte.



was caused by graphene and water vapor rather than by the electrolyte.

CV of BC and UGCC were performed employing 1M of potassium ferricyanide electrolyte at the scan rate of 25 mV/s and temperature difference of  $\Delta T = 60^\circ\text{C}$  (Figure 6). CV of BC show reduction peak of Fe(III)/Fe(II) at 0.1 V and oxidation peak of Fe(II)/Fe(III) at 0.55 V vs. Ag/AgCl [27]. The peak at  $-0.3$  V correspond to oxidation of Cu into  $\text{Cu}_2\text{O}$ . CV of UGCC electrode resulted in identical peaks as that of BC with reduced peak height due to presence of thin graphene layer. Inset CV of GCC showed one oxidation peak at 0.85 V corresponding to Fe(II)/Fe(III) and the copper oxidation peak had disappeared as shown in Figure 6. The diffusion coefficient of the electrolyte on BC, UGCC, GCC electrodes were  $3.19 \times 10^{-3} \text{ cm}^2/\text{s}$ ,  $3.12 \times 10^{-3} \text{ cm}^2/\text{s}$ ,  $4.05 \times 10^{-3} \text{ cm}^2/\text{s}$  as calculated using Randles-Sevcik Equation [7]:

$$i_p = (2.69 \times 10^5) n^{3/5} A D^{1/2} \nu^{1/2} C \quad (4)$$

where, the constant  $2.69 \times 10^5$  is calculated at  $25^\circ\text{C}$ ,  $i_p$  = peak current in ampere,  $n$  = number of electrons,  $A$  = area of the electrode in  $\text{cm}^2$ .

## REFERENCES

- Dupont MF, MacFarlane DR, Pringle JM. Thermo-electrochemical cells for waste heat harvesting-progress and perspectives. *Chem. Commun.* (2017) 53:6288–302. doi: 10.1039/C7CC02160G
- Siddique ARM, Mahmud S, Heyst BV. A review of the state of the science on wearable thermoelectric power generators (TEGs) and their existing challenges. *Renew Sustain Energy Rev.* (2017) 73:730–44. doi: 10.1016/j.rser.2017.01.177
- Quickenden TI, MuaY. A review of power generation in aqueous thermogalvanic cells. *J Electrochem Soc.* (1995) 142:3985–94. doi: 10.1149/1.2048446
- Salazar PF, Kumar S, Cola BA. Design and optimization of thermo-electrochemical cells. *J Appl Electrochem.* (2014) 44:325–36. doi: 10.1007/s10800-013-0638-y

$D$  = diffusion coefficient in  $\text{cm}^2/\text{s}$ ,  $C$  = concentration of the species in  $\text{mol}/\text{cm}^3$ ,  $\nu$  = scan rate in mV/s.  $D$  values of BC and UGCC were close whereas GCC showed approximately 1.26 times higher value. This clearly indicated peeling of graphene coating on prolonged usage of the device and the copper getting exposed to the electrolyte solution.

## SUMMARY

In summary, we report conversion of low-grade waste heat into electricity by thermocells connected in series based on cost effective graphene coated copper electrodes displaying relatively high efficiency of thermal energy harvesting. The maximum power output of  $49.2 \text{ W}/\text{m}^2$  and relative carnot efficiency of 20.2% is obtained at  $60^\circ\text{C}$  of inter electrode temperature difference from the device. EIS analysis showed the importance of reducing the mass transfer and ion transfer resistance to improve the efficiency of the device. Degradation studies confirmed mild oxidation of copper foil due to corrosion in the presence of electrolyte.

## AUTHOR CONTRIBUTIONS

MS performed EIS analysis; EI performed electrochemical experiments and fabricated the device; VS performed analysis of LSV; SH generated the idea and wrote the manuscript.

## ACKNOWLEDGMENTS

This work was supported by Department of Science and Technology-Science and Engineering Research board (EMR2014001159).

## SUPPLEMENTARY MATERIAL

The Supplementary Material for this article can be found online at: <https://www.frontiersin.org/articles/10.3389/fphy.2018.00035/full#supplementary-material>

Electrochemical performance data, lower limit of mass transfer coefficient, the energy conversion efficiency, relative carnot efficiency of the device at different inter electrode temperature are provided in Supporting Information.

- Salazar PF, Stephens ST, Kazim AH, Pringle JM, Cola BA. Enhanced thermo-electrochemical power using carbon nanotube additives in ionic liquid redox electrolytes. *J Mater Chem A* (2014) 2:20676–82. doi: 10.1039/C4TA04749D
- Kazima AH, Cola BA. Electrochemical characterization of carbon nanotubes and poly(3,4-ethylenedioxythiophene)-poly(styrenesulfonate) composite aqueous electrolyte for thermo-electrochemical cells. *J Electrochem Soc.* (2016) 163:F867–71. doi: 10.1149/2.0981608jes
- Bard AJ, Faulkner LR. *Electrochemical Methods: Fundamentals and Applications*. New York, NY: Wiley (1980).
- Quickenden TI, Vernon CF. Thermogalvanic conversion of heat to electricity. *Solar Energy* (1986) 36:63–72. doi: 10.1016/0038-092X(86)90061-7
- Qian W, Cao M, Xie F, Dong C. Thermo-electrochemical cells based on Carbon Nanotube electrodes by electrophoretic deposition. *Nano-Micro Lett.* (2016) 8:240–6. doi: 10.1007/s40820-016-0082-8

10. Hu R, Cola BA, Haram N, Barisci JN, Lee S, Stoughton S, et al. Harvesting thermal energy using a Carbon-Nanotube based thermoelectrochemical cell. *Nano Lett.* (2010) **10**:838–46. doi: 10.1021/nl903267n
11. Burrows B. Discharge behavior of redox thermogalvanic cells. *J Electrochem Soc.* (1976) **123**:154–9. doi: 10.1149/1.2132776
12. Mua Y, Quickenden TI. Power conversion efficiency, electrode separation, and overpotential in the ferricyanide/ferricyanide thermogalvanic cell. *J Electrochem Soc.* (1996) **143**:2558–63. doi: 10.1149/1.1837047
13. Shindo K, Arakawa M, Hirai T. Effect of non-graphitized carbon electrodes on the electrochemical characteristics of a thermocell with a Br<sub>2</sub>/Br<sup>-</sup> redox couple. *J Power Sourc.* (1998) **70**:228–34. doi: 10.1016/S0378-7753(97)02676-1
14. deBethune AJ, Licht TS, Swendeman N. The temperature coefficients of electrode potentials the isothermal and thermal coefficients—the standard ionic entropy of electrochemical transport of the hydrogen ion. *J Electrochem Soc.* (1959) **106**:616–25. doi: 10.1149/1.2427448
15. Kang TJ, Fang S, Kozlov ME, Haines CS, Li N, Kim YH, et al. Electrical power from nanotube and graphene electrochemical thermal energy harvesters. *Adv Funct Mater.* (2012) **22**:477–89. doi: 10.1002/adfm.201101639
16. Yang HD, Tufa LT, Bae KM, Kang TJ. A tubing shaped, flexible thermal energy harvester based on a carbon nanotube sheet electrode. *Carbon* (2015) **86**:118–23. doi: 10.1016/j.carbon.2015.01.037
17. Bae KM, Yang HD, Tufa LT, Kang TJ. Thermobattery based on CNT coated carbon textile and thermoelectric electrolyte. *Int. J. Precis. Eng. Manuf.* (2015) **16**:1245–50. doi: 10.1007/s12541-015-0162-6
18. Im H, Kim T, Song H, Choi J, Park JS, Robles RO, et al. High-efficiency electrochemical thermal energy harvester using carbon nanotube aerogel sheet electrodes. *Nat Commun.* (2016) **7**:10600. doi: 10.1038/ncomms10600
19. Sindhuja M, Lohith B, Sudha V, Manjunath G, Harinipriya S. Low grade thermal energy harvester using graphene based-thermocells. *Mater Res Exp.* (2017) **4**:075513. doi: 10.1088/2053-1591/aa7afa
20. Swathi M, Saini A, Khaleeq S, Patel R, Usmani B, Harinipriya S, et al. Thermocells of carbon material electrodes and its performance characteristics. *J Mater Res Technol.* (2013) **2**:165–81. doi: 10.1016/j.jmrt.2013.01.005
21. Dong X, Wang K, Zhao C, Qian X, Chen S, Li Z, et al. Direct synthesis of RGO/Cu<sub>2</sub>O composite films on Cu foil for supercapacitors. *J Alloys Compounds* (2014) **586**:745–53. doi: 10.1016/j.jallcom.2013.10.078
22. Lamberti A, Destro M, Bianco S, Quaglio M, Chiodoni A, Pirri CF, et al. Facile fabrication of cuprous oxide nanocomposite anode films for flexible Li-ion batteries via thermal oxidation. *Electrochim. Acta* (2012) **70**:62–8. doi: 10.1016/j.electacta.2012.03.025
23. Veerapandian M, Subbiah R, Lim GS, Park SH, Yun KS, Lee MH. Copper-glucosamine microcubes: synthesis, characterization, and C-reactive protein detection. *Langmuir* (2011) **27**:8934–42. doi: 10.1021/la2009495
24. Rafiqi FA, Majid K. Removal of copper from aqueous solution using polyaniline and polyaniline/ferricyanide composite. *J Environ Chem Eng.* (2015) **3**:2492–501. doi: 10.1016/j.jece.2015.09.013
25. Shankar S, Rhim JW. Preparation of nanocellulose from microcrystalline cellulose: the effect on the performance and properties of agar-based composite films. *Carbohydr Polym.* (2016) **135**:18–26. doi: 10.1016/j.carbpol.2015.08.082
26. Kanmani P, Rhim JW. Properties and characterization of bionanocomposite films prepared with various biopolymers and ZnO nanoparticles. *Carbohydr Polym.* (2014) **102**:708–16. doi: 10.1016/j.carbpol.2013.10.099
27. Radhi MM, Jaffar Al-Mulla EA, Tan WT. Electrochemical characterization of the redox couple of Fe(III)/Fe(II) mediated by grafted polymer electrode. *Res Chem Intermed.* (2012) **40**:179–92. doi: 10.1007/s11164-012-0954-6

**Conflict of Interest Statement:** The authors declare that the research was conducted in the absence of any commercial or financial relationships that could be construed as a potential conflict of interest.

Copyright © 2018 Sindhuja, Indubala, Sudha and Harinipriya. This is an open-access article distributed under the terms of the Creative Commons Attribution License (CC BY). The use, distribution or reproduction in other forums is permitted, provided the original author(s) and the copyright owner are credited and that the original publication in this journal is cited, in accordance with accepted academic practice. No use, distribution or reproduction is permitted which does not comply with these terms.